water

MDPI

Article

Cross-Linked Magnetic Chitosan/Activated Biochar for Removal of Emerging Micropollutants from Water: Optimization by the Artificial Neural Network

Amin Mojiri [1,*], Reza Andasht Kazeroon [2] and Ali Gholami [3]

[1] Department of Civil and Environmental Engineering, Hiroshima University, 1-4-1 Kagamiyama, Higashihiroshima 739-8527, Japan
[2] Faculty of Civil Engineering, University Technology Mara (UiTM), Shah Alam 40450, Selangor, Malaysia; reza.andasht@gmail.com
[3] Department of Soil Science, Ahvaz Branch, Islamic Azad University, Ahvaz 6165765675, Iran; ali.gholami54@gmail.com
* Correspondence: amin.mojiri@gmail.com

Received: 18 February 2019; Accepted: 13 March 2019; Published: 17 March 2019

Abstract: One of the most important types of emerging micropollutants is the pharmaceutical micropollutant. Pharmaceutical micropollutants are usually identified in several environmental compartments, so the removal of pharmaceutical micropollutants is a global concern. This study aimed to remove diclofenac (DCF), ibuprofen (IBP), and naproxen (NPX) from the aqueous solution via cross-linked magnetic chitosan/activated biochar (CMCAB). Two independent factors—pH (4–8) and a concentration of emerging micropollutants (0.5–3 mg/L)—were monitored in this study. Adsorbent dosage (g/L) and adsorption time (h) were fixed at 1.6 and 1.5, respectively, based on the results of preliminary experiments. At a pH of 6.0 and an initial micropollutant (MP) concentration of 2.5 mg/L, 2.41 mg/L (96.4%) of DCF, 2.47 mg/L (98.8%) of IBP, and 2.38 mg/L (95.2%) of NPX were removed. Optimization was done by an artificial neural network (ANN), which proved to be reasonable at optimizing emerging micropollutant elimination by CMCAB as indicated by the high R^2 values and reasonable mean square errors (MSE). Adsorption isotherm studies indicated that both Langmuir and Freundlich isotherms were able to explain micropollutant adsorption by CMCAB. Finally, desorption tests proved that cross-linked magnetic chitosan/activated biochar might be employed for at least eight adsorption-desorption cycles.

Keywords: chitosan; diclofenac; ibuprofen; magnetic biochar; naproxen

1. Introduction

Emerging micropollutants or organic micropollutants exist in the environment at trace concentrations, and their impact on the human health and the environment are presently unknown. These pollutants are contained in polycyclic aromatic hydrocarbons (PAH), personal care products, pharmaceuticals, pesticides, industrial chemicals, and metallic trace elements [1]. Pharmaceutical micropollutants are commonly found in various environmental compartments. The growing use of pharmaceuticals is raises questions regarding their potential risk to human health, the environment, and water quality [2]. Diclofenac, ibuprofen, and naproxen are non-steroidal anti-inflammatory drugs (NSAIDs), which are a commonly consumed class of pharmaceuticals [3]. All pharmaceuticals belonging to this group are acidic in nature with pKa values in the range of 3–5 [4].

Among the different non-steroidal anti-inflammatory drugs, diclofenac is widely applied. Diclofenac (Figure 1; 2-((2,6-dichlorophenyl)amino)phenylacetic-acid) has been stated to cause chronic results such as renal and gastrointestinal tissue damage in some vertebrates [5]. Ibuprofen (Figure 1;

2-(4-Isobutylphenyl)propionic acid) is applied for the treatment of pain and inflammation and dropping of a fever [6]. Naproxen (Figure 1) enters aquatic environments chiefly over the effluents of wastewater treatment plants. It is categorized as a high-priority pharmaceutical. Naproxen might affect living organisms and diminish the biodiversity of natural environmental communities because of its biological activities [7]. Mostly, conventional wastewater treatment methods fail to eliminate pharmaceuticals totally from the water [2]. One of the most promising ways to remove emerging micropollutants is by using adsorbents. Biochar and chitosan are low-cost adsorbents which have been previously used in the literature to remove micropollutants from water [8,9].

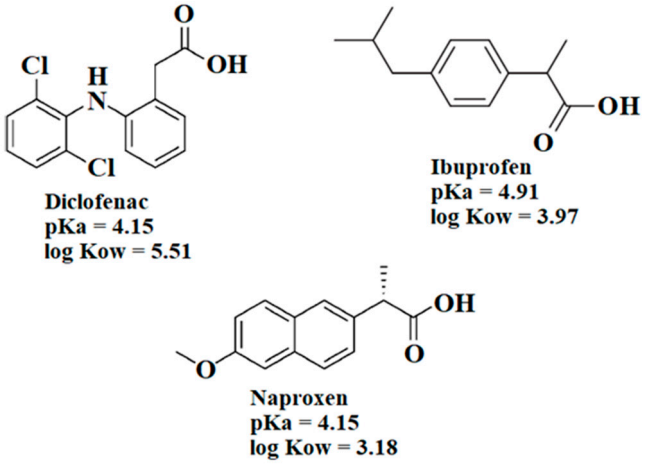

Figure 1. Structures of the studied organic micropollutants [10,11].

Chitosan is one of the biopolymers that is derived from chitin; chitin is a natural amino polysaccharide and is composed primarily of repeating β-(1,4)-2-amino-2-deoxy-d-glucose (or d-glucosamine) units. The benefits of chitosan include its low cost, ease of polymerization and functionalization, and good stability [12]. Amouzgar and Salamatinia [8] stated that chitosan has certain capabilities for removing emerging micropollutants from water. Another low-cost adsorbent is biochar.

Thermochemical decomposition procedures transform biomass materials to syngas, bio-oil, and biochar. Biochar is low cost, environmentally friendly, and can be applied for a variety of purposes [13]. Quesada et al. [14] stated that using biochar as a low-cost material is a promising way to eliminate pharmaceuticals from wastewater. Sizmur et al. [15] stated that the activation process improves the surface area and porosity of biochar, so its adsorption capacity might be increased. Hence, this study aimed to produce a new cross-linked magnetic chitosan/activated biochar to remove emerging micropollutants and to optimize the removal efficiency using an artificial neural network (ANN). This experiment design and its optimization process have not been previously reported in the literature.

2. Materials and Methods

2.1. Materials

In this study, biochar was extracted from agricultural residues. Chitosan (medium molecular weight; code: 07947-52), diclofenac sodium (DCF; $C_{14}H_{10}Cl_2NNaO_2$; 98%; molecular weight = 294.05 g/mol), ibuprofen (IBP; $C_{13}H_{18}O_2$; 98%; molecular weight = 206.3 g/mol), and naproxen (NPX; 98%; $C_{14}H_{14}O_3$; molecular weight = 230.2 g/mol) were obtained from Sigma–Aldrich in the analytical purity and applied in the experiments directly without any further purification. Chloroform, acetone, and methanol (99.5% mass purity) were from Merck.

2.2. Producing Cross-Linked Magnetic Chitosan/Activated Biochar (CMCAB)

Based on the method by Liu et al. [16] in the first step, magnetic fluid was prepared by a co-precipitation technique. Fe^{2+} and Fe^{3+} (molar ratio 2:3) solution was placed into a beaker using a stirrer at 55 °C, then NaOH solution was added dropwise with continuous stirring for almost 15 min until the pH got to 9.0. After altering the temperature of the reaction vessels to 65 °C, 0.8 mL Tween 80 was augmented into the mixture using a stirrer for 30–40 min, and the pH value was adjusted to 7.0. After that, the product was washed with distilled water three times and was dispersed in an ultrasonic device for 40 min. Finally, the solution was diluted to gain magnetic fluid (40 g L^{-1}).

In the second step, the activated biochar was produced. Biochar extracted from agricultural residues was done by an activation process with 4 M NaOH for 2 h and then dried for 12 h at 105 °C. Then, the biochar was separated from the NaOH solution via a Buchner filter funnel, heated at 800 °C for 2 h under a 2 L/min nitrogen gas flow, and then let to cool at a rate of 10 °C /min. The activated biochar was washed consecutively with deionized (DI) water and 0.1 M HCl to attain pH 7 and dried again at 105 °C. As a final point, the activated biochar was crushed and sieved through a 200-mesh (74 µm) sieve [17].

Finally, to achieve the cross-linked magnetic chitosan/activated biochar, 5.0 g of chitosan was dissolved in 250 mL 2% acetic solution with stirring. Next, 25 mL of magnetic fluid was added dropwise into the solution with constant stirring for 30 min in a water bath at 50 °C. Then, 5.0 g activated biochar was augmented with continuous stirring for another 60 min. Afterward, 6 mL of glutaraldehyde was injected into the reaction system to produce a gel and the pH of the reaction system was adjusted to 8.0–10.0. As a final point, the mixture was retained in a water bath for 1 h. The precipitate was washed till the pH touched about 7 and was dried at 60 °C and sieved [16]. Table 1 shows the features of the cross-linked magnetic chitosan/activated biochar (CMCAB). The CMCAB features were monitored by the Autosorb (Quantachrome AS1wintm, version 2.02, Quantachrome Instruments, Boynton Beach, FL, USA). In terms of the BET technique, the specific surface area and pore size distribution of CMCAB with the specific surface area and pore size distribution analyzers were determined under the conditions of liquid nitrogen temperature. The zeta potential of the CMCAB was analyzed by the zeta potential meter (Zetasizer nano-ZS90, Malvern Panalytical Ltd, Malvern, UK) at 25 °C in different pH (3–9).

Table 1. Characteristics of the cross-linked magnetic chitosan/activated biochar (CMCAB).

Parameter	Unit	Value
BET surface area	m^2/g	502
Langmuir surface area	m^2/g	796
BJH method cumulative adsorption surface area	m^2/g	12.7
Single point surface area at p/p_o 0.2027	m^2/g	422
Micropore area	m^2/g	217
Single point total pore volume of pores less than 1265.1476 in diameter at p/p_o 0.9845	cc/g	0.4
Micropore volume	cc/g	0.11
Average pore diameter (4 v/a by Langmuir)	A	8.9
BJH adsorption average pore diameter (4 v/a)	A	31.2

2.3. Producing the Synthetic Aqueous Solution and Experiment Design

Stock solutions of organic micropollutants were prepared in acetone, chloroform, or methanol as described by Sühnholz et al. [18]. In this study, the initial concentration of organic micropollutants ranged from 0.5 mg/L [19] to 3 mg/L [20]. The pH was varied from 4 to 8 [21]. Based on preliminary experiments, the adsorption time (h) was fixed at 1.5, which is in line with selected ranges by

Kim et al. [9]. Based on preliminary experiments, the adsorbent dosage was fixed at 1.6 g/L, which is in line with the findings of Wu et al. [22]. Based on preliminary experiments, each run was carried out at room temperature (25 ± 1 °C) using a shaker with 300 rpm shaking speed for all conditions [17,23]. A schematic of the current study is shown in Figure 2.

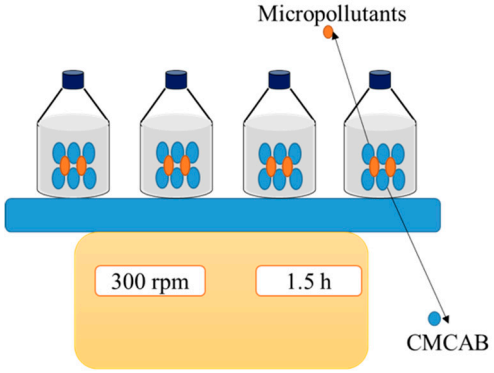

Figure 2. Schematic of experiments.

2.4. Analytical Techniques

All analytical methods were conducted on the basis of the standard methods [24]. The concentrations of emerging micropollutants were tested via ultraviolet spectra and measured by a high-pressure liquid chromatography (HPLC) (LC-20AT, Shimadzu International Trading (Shanghai) Co., Ltd., Tokyo, Japan). The analytical techniques for diclofenac (DCF), ibuprofen (IBP), and naproxen (NPX) were obtained from the literature [25]. The applied mobile phase contained a mixture of acetonitrile and 0.2% formic acid in water (60:40, v/v) at a flow rate of 0.8 mL min^{-1}. The concentrations of DCF, IBP, and NPX were tested using a UV detector at the wavelengths of 200, 200, and 230 nm.

2.5. Optimization Analysis using an Artificial Neural Network (ANN)

The percentage of micropollutants (MP) eliminated from the solution was estimated using Equation (1)

$$\text{Removal } \% = \frac{C_i - C_f}{C_i} \times 100 \quad (1)$$

The initial concentration of MP and the final concentration of MP are denoted by C_i and C_f, respectively.

MATLAB R2015a software (R2015a, Mathsworks, Natick, MA, USA) was applied to model the adsorption procedure on the basis of an ANN. Figure 3 displays the topology for the ANN and the variation of parameters in this study. The two neurons in the input layer represent pH (4–8) and micropollutant concentration (0.5–3 mg/L). There were four neurons in the hidden layer and one neuron in the output layer (removal efficiency) for modeling each micropollutant elimination. A total of 50 experimental results applied to model the network were divided randomly into training (60%), validation (20%), and test (20%) sets [26]. The ANN performance was defined based on the values of the mean squared error (MSE) and coefficient of determination (R^2). They were respectively evaluated using Equations (2) and (3). Levenberg–Marquardt (LM) was applied to train the model, and validation was stopped when the maximum validation failures were equal to zero.

$$\text{MSE} = \frac{1}{N}\sum_{i=1}^{N}\left(\left|y_{prd,i} - y_{exp,i}\right|\right)^2, \quad (2)$$

$$R^2 = 1 - \frac{\sum_{i=1}^{N}\left(y_{prd,\,i,}\, y_{exp,i}\right)}{\sum_{i=1}^{N} y_{prd,i} - y_m}, \quad (3)$$

In Equations (4) and (5), $y_{prd,i}$ refers to the predicted value using the ANN model, $y_{exp,i}$ is the experimental value, N is the number of datapoints, and y_m indicates the average of the experimental values.

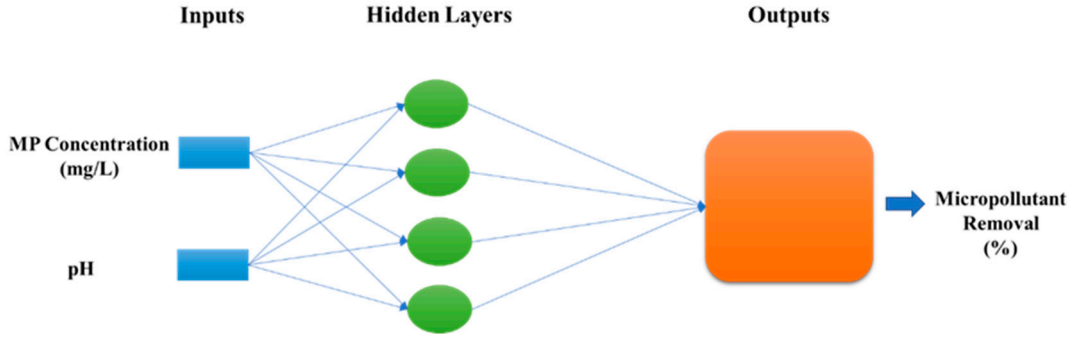

Figure 3. Schematic of an artificial neural network (ANN) design.

2.6. Adsorption Isotherm Study

Batch adsorption studies were done via different dosages (1–7 g/L) of the CMCAB in a fixed MP concentration (2.5 mg/L), pH (6), and adsorption time (30 min). Beakers with working volumes of 100 mL were shaken at 300 rpm for 30 min.

The capacity of adsorption (mg/g) was estimated via the following Equation (4) [27]:

$$q_e = \frac{(C_0 - C_{eq})V}{m_s}, \quad (4)$$

where the initial micropollutant (MP) concentration is denoted by q_e, C_{eq} is the MP concentration (mg L^{-1}) at equilibrium, the volume of solution (L) is represented by V, and m_s is the mass of the adsorbent (g).

2.7. Regeneration and Desorption Study

Regeneration studies were carried out to monitor the economic usability of the CMCAB adsorbent. The adsorbent was regenerated by soaking in 100 mL methanol for 2–3 h in batch experiments and then washed using distilled water in order to consider the desorption and regeneration of the CMCAB. Eight adsorption/desorption cycles were carried out. After every cycle, the residual concentration of MPs was monitored [28].

3. Results and Discussion

The efficiency of the removal of emerging micropollutants via cross-linked magnetic chitosan/activated biochar (CMCAB) is shown in Table 2. Figure 4 shows the FTIR results of CMCAB.

In the FTIR results of chitosan (Figure 4a), peaks 3398 and 2913 can be attributed to O–H and C–H, respectively [29]; peak 1613 may be related to C = O [30]. N–H and CH–OH could explain peaks 1584 and 1401, respectively [29]; and peak 837 is attributed to CH groups [30]. In the FTIR results of activated biochar (Figure 4b), peaks 3207 and 2981 are attributed to O–H and C–H, respectively, while peaks 1608 and 1513 may be related to C = O and C = C, respectively [31]. C–O and O–H could be responsible for peak 1201 [31], and peak 842 is attributed to C–H groups [30]. In the FTIR results of the CMCAB (Figure 4c), peaks 3496 and 2915 are attributed to –OH (or –NH) and C–H, respectively [29]. Peaks C = N and C–O could explain peaks 1638 and 1043, respectively [32,33] and peaks 771 and 573 are attributed to Fe–O [32,33]. The zeta potential of CMCAB is shown in Figure 5. Based on Figure 5, the zeta potential of CMCAB was positive in pH (3) to (5) it is in line with finding of Liu et al. [16] and Zhang et al. [33]. Zeta potentials (mV) were 19, 16 and 1 in pH (3), pH (4) and pH (5), respectively. After that zeta potential became negative which could be supported by findings of Zhang et al. [33].

Zeta potentials (mV) were −5, −6, −8 and −11 in pH (6), pH (7), pH (8), and pH (9), respectively. It should be mentioned that the zero point during the zeta potential testing for CMCAB was reached at 5.2 of pH, which could be supported by findings of Liu et al. [16].

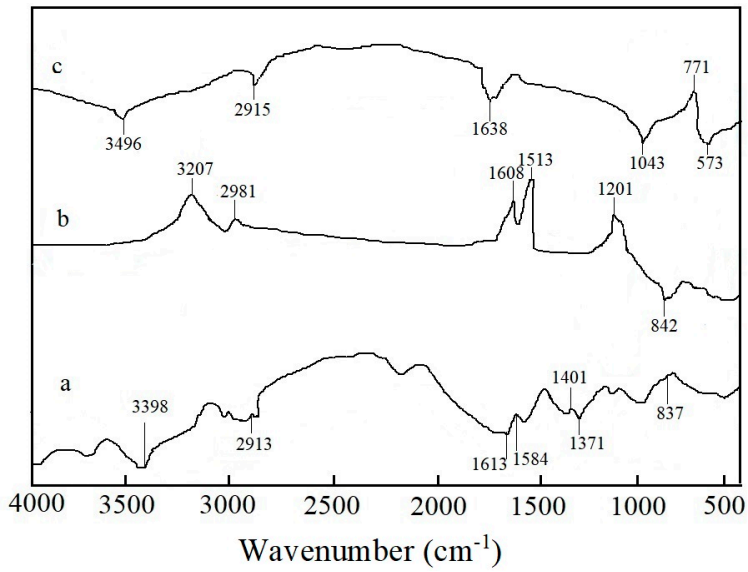

Figure 4. FTIR images of chitosan (**a**), activated Biochar (**b**), and cross-linked magnetic chitosan/activated biochar (CMCAB) (**c**).

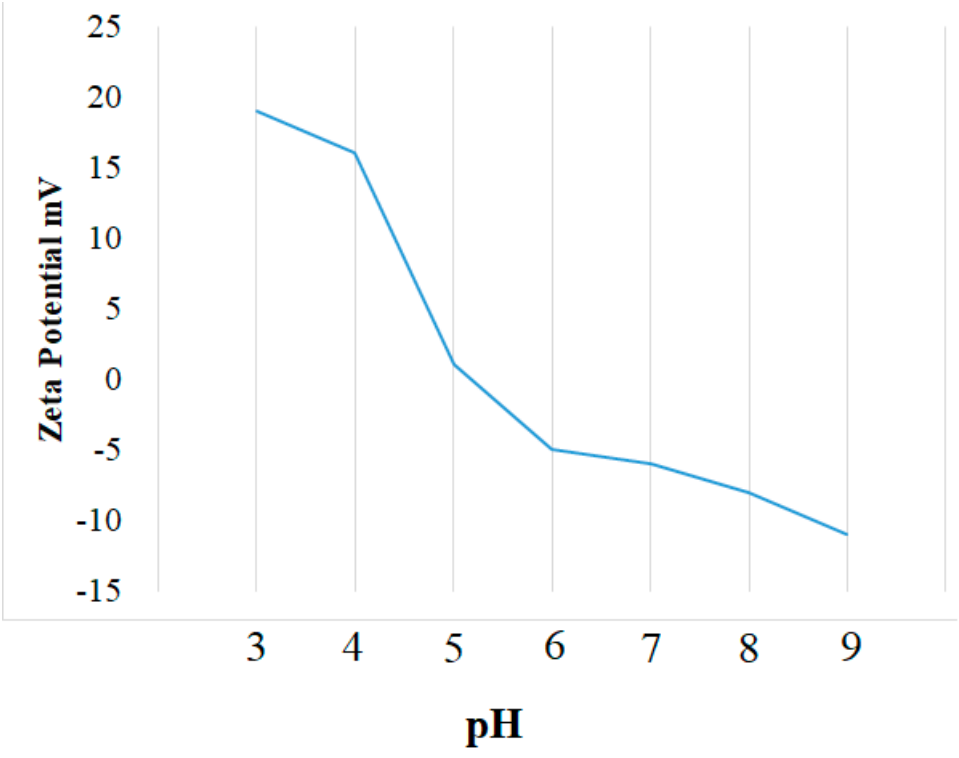

Figure 5. The zeta potential of CMCAB in pH (3–9).

Table 2. Elimination of diclofenac (DCF), ibuprofen (IBP), and naproxen (NPX) by CMCAB.

Run	pH	Initial Concentration (mg/L)	DCF Removal		IBP Removal		NPX Removal	
			(%)	(mg/L)	(%)	(mg/L)	(%)	(mg/L)
1	4.00	0.5	63.7	0.319	65.2	0.326	64.7	0.324
2	4.00	1.0	64.1	0.641	65.8	0.658	64.9	0.649
3	4.00	1.5	64.7	0.971	66.6	0.999	65.8	0.987
4	4.00	2.0	66.2	1.324	66.6	1.332	65.4	1.308
5	4.00	2.5	67.9	1.698	67.5	1.688	66.6	1.665
6	4.00	3.0	66.6	1.998	66.2	1.986	65.7	1.971
7	4.50	0.5	73.2	0.366	74.1	0.371	73.1	0.366
8	4.50	1.0	73.5	0.735	74.8	0.748	73.4	0.734
9	4.50	2.0	73.5	1.470	75.4	1.508	74.9	1.498
10	4.50	2.5	75.9	1.898	75.6	1.890	75.5	1.888
11	4.50	3.0	76.3	2.289	77.1	2.313	75.4	2.262
12	5.00	0.5	81.3	0.407	82.1	0.411	81.6	0.408
13	5.00	1.0	81.6	0.816	82.7	0.827	81.6	0.816
14	5.00	1.5	82.1	1.232	84.9	1.274	81.7	1.226
15	5.00	2.0	82.1	1.642	84.9	1.698	82.2	1.644
16	5.00	2.5	83.0	2.075	84.9	2.123	82.4	2.060
17	5.00	3.0	83.8	2.514	84.7	2.541	81.9	2.457
18	5.50	0.5	87.6	0.438	88.2	0.441	86.9	0.435
19	5.50	1.0	88.2	0.882	88.6	0.886	87.3	0.873
20	5.50	2.0	88.1	1.762	89.1	1.782	87.5	1.750
21	5.50	2.5	89.1	2.228	90.4	2.260	88.2	2.205
22	5.50	3.0	88.6	2.658	90.8	2.724	87.5	2.625
23	6.00	0.5	93.6	0.468	94.8	0.474	91.6	0.458
24	6.00	1.0	93.9	0.939	94.6	0.946	93.2	0.932
25	6.00	1.5	94.7	1.421	97.3	1.460	93.5	1.403
26	6.00	2.0	95.0	1.900	97.8	1.956	94.1	1.882
27	6.00	2.5	96.4	2.410	98.8	2.470	95.2	2.380
28	6.00	3.0	96.1	2.883	98.2	2.946	94.8	2.844
29	6.50	0.5	83.8	0.419	84.0	0.420	82.8	0.414
30	6.50	1.0	84.2	0.842	84.6	0.846	82.6	0.826
31	6.50	2.0	85.1	1.702	86.3	1.726	83.1	1.662
32	6.50	2.5	85.9	2.148	87.4	2.185	83.6	2.090
33	6.50	3.0	85.2	2.556	87.3	2.619	83.2	2.496
34	7.00	0.5	61.0	0.305	62.6	0.313	60.3	0.302
35	7.00	1.0	61.3	0.613	63.5	0.635	60.3	0.603
36	7.00	1.5	61.9	0.929	63.2	0.948	60.8	0.912
37	7.00	2.0	61.9	1.238	64.3	1.286	61.0	1.220
38	7.00	2.5	62.8	1.570	64.8	1.620	61.4	1.535
39	7.00	3.0	62.5	1.875	64.3	1.929	61.4	1.842
40	7.50	0.5	54.7	0.274	52.6	0.263	51.9	0.260

Table 2. *Cont.*

Run	pH	Initial Concentration (mg/L)	DCF Removal		IBP Removal		NPX Removal	
			(%)	(mg/L)	(%)	(mg/L)	(%)	(mg/L)
41	7.50	1.0	54.7	0.547	53.1	0.531	52.2	0.522
42	7.50	2.0	53.6	1.072	52.7	1.054	51.1	1.022
43	7.50	2.5	53.1	1.328	52.7	1.318	51.2	1.280
44	7.50	3.0	52.8	1.584	51.8	1.554	50.7	1.521
45	8.00	0.5	41.7	0.209	42.4	0.212	39.6	0.198
46	8.00	1.0	40.1	0.401	41.6	0.416	39.6	0.396
47	8.00	1.5	39.2	0.588	41.2	0.618	39.1	0.587
48	8.00	2.0	38.7	0.774	40.7	0.814	38.7	0.774
49	8.00	2.5	39.8	0.995	40.9	1.023	39.2	0.980
50	8.00	3.0	40.7	1.221	40.2	1.206	39.6	1.188

3.1. Emerging Micropollutants Removal

Based on Table 2 and Figure 6a, the maximum removal of diclofenac (DCF) was 96.4% (2.41 mg/L) at pH 6 and an initial concentration of 2.5 mg/L, while the minimum removal of DCF was 38.7% (0.77 mg/L) at pH 8 and an initial concentration of 2 mg/L. Liang et al. [34] reported 70% DCF removal via magnetic amine-functionalized chitosan. Lonappan et al. [35] reported 42% to 98% DCF removal in the presence of a high dosage of biochar microparticles (2–20 g/L). Based on Table 2 and Figure 6b, the optimum elimination of ibuprofen (IBP) was 98.8% (2.47 mg/L) at pH 6 and an initial concentration of 2.5 mg/L, and the minimum removal of IBP was 40.2% (1.20 mg/L) at pH 8 and an initial concentration of 3 mg/L. Chakraborty et al. [36] removed 82% to 91% of IBP via bi-directional activated biochar over high contact time (12–18 h). Paradis-Tanguay et al. [37] removed 70% of IBP using chitosan/polyethylene oxide (PEO) electrospun nanofibers. Based on Table 2 and Figure 6c, the maximum removal of naproxen (NPX) was 95.2% (2.38 mg/L) at pH 6 and an initial concentration of 2.5 mg/L, while the minimum removal of NPX was 38.7% (0.77 mg/L) at pH 8 and an initial the concentration of 2 mg/L. Jung et al. [38] reported 97% NPX removal via a combined coagulation/biochar method. Based on Table 2, the removal effectiveness slightly increased with increasing initial concentration of emerging micropollutants from 0.5 mg/L to 2.5 mg/L.

As shown in Table 2 and Figure 6, the elimination efficiencies of the emerging micropollutants increased with increasing the pH from 4 to 6, and maximum micropollutant removal occurred at pH 6, whereas at pH 5–6, the net surface charge is positive and ion repulsion still exists [39]. Then, the removal effectiveness decreased from pH 6 to 8. Gu et al. [40] reported that the pH of a solution has a significant impact on the adsorption procedure because the surface charge of the adsorbent might be changed in the varied pH. Rafati et al. [41] reported that the maximum removal of emerging micropollutants using an adsorption method was reached at pH 6. The diminishing competition of H^+ ions at increasing pH improved the adsorption to reach the maximum removal at pH 6. Besha et al. [42] expressed that elimination of acidic pharmaceuticals such as ibuprofen, naproxen, and diclofenac might be enriched at slightly acidic pH; this is probably because of the hydrophobicity of these compounds.

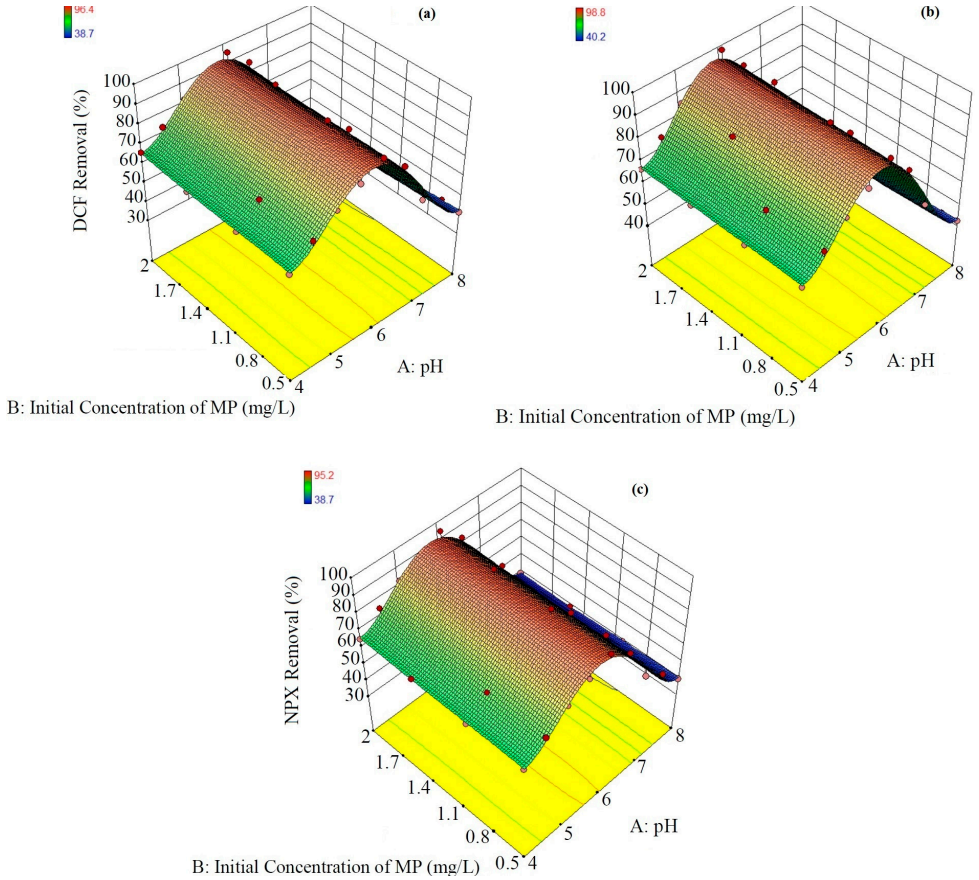

Figure 6. Removal efficiencies for diclofenac (**a**), ibuprofen (**b**), and naproxen (**c**).

3.2. Optimization using an ANN

Artificial neural networks (ANN) are computer techniques on the basis of models of the human brain's biological activities, such as the capability to learn, think, solve issues and remember. Neural network models contain weights and neurons. The neural network contains a combined structure comprising an input layer, intermediate layer (hidden layer), and an output layer. Each layer contains of simple processing features called neurons. The mean square error (MSE) and R^2 values (Table 3) for DCF, IBP, and NPX elimination are shown in Table 3. Figure 7 indicates the best setting of the ANN. Figure 8 displays the change in the MSE values by Levenberg–Marquardt (LM) through selecting various functions such as pure linear, transig, and log sigmoid. This figure also specifies that the training was completed after 68, 25, and 34 epochs for DCF (a), IBP (b), and NPX (c), respectively. These consequences also proved that the ANN model was well-trained at the end of the training phase [43,44].

The high values of R^2 (Figure 9) indicated an excellent agreement between the ANN predicted data and the actual data [43].

Table 3. R^2 and MSE values for the removal of each pollutant in the selection of the best model.

Parameter	R^2			MSE		
	Training	Validation	Test	Training	Validation	Test
For DCF Removal	0.999	0.998	0.998	0.220	0.837	0.212
For IBP Removal	0.998	0.998	0.998	0.697	2.929	0.829
For NPX Removal	0.999	0.999	0.999	0.235	0.276	0.371

Figure 7. Artificial neural network (ANN) settings for the best model for diclofenac (**a**), ibuprofen (**b**), and naproxen (**c**).

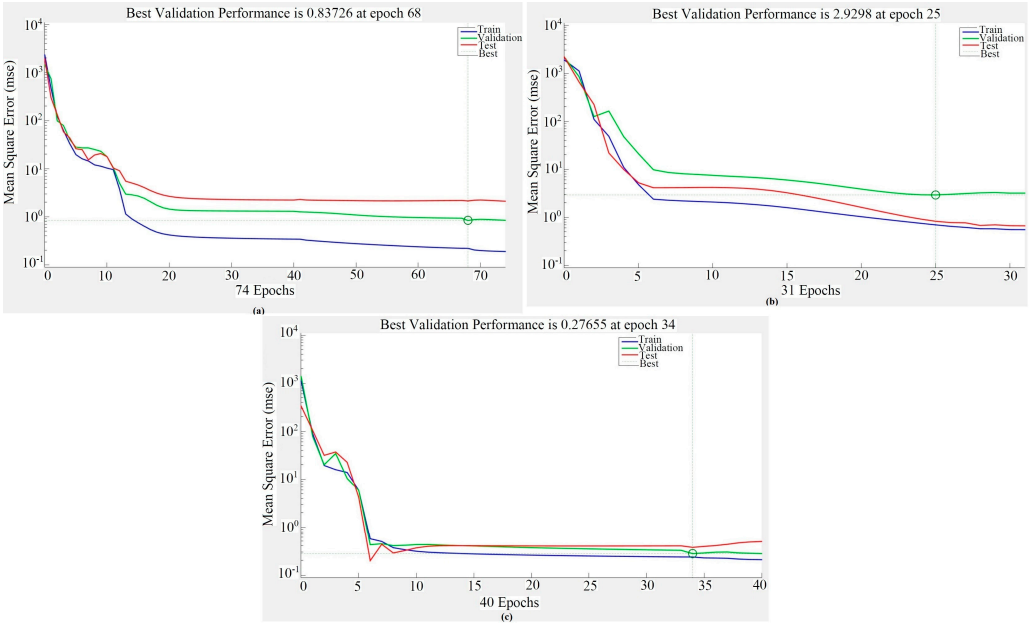

Figure 8. Mean square error (MSE) versus the number of epochs for diclofenac (**a**), ibuprofen (**b**), and naproxen (**c**).

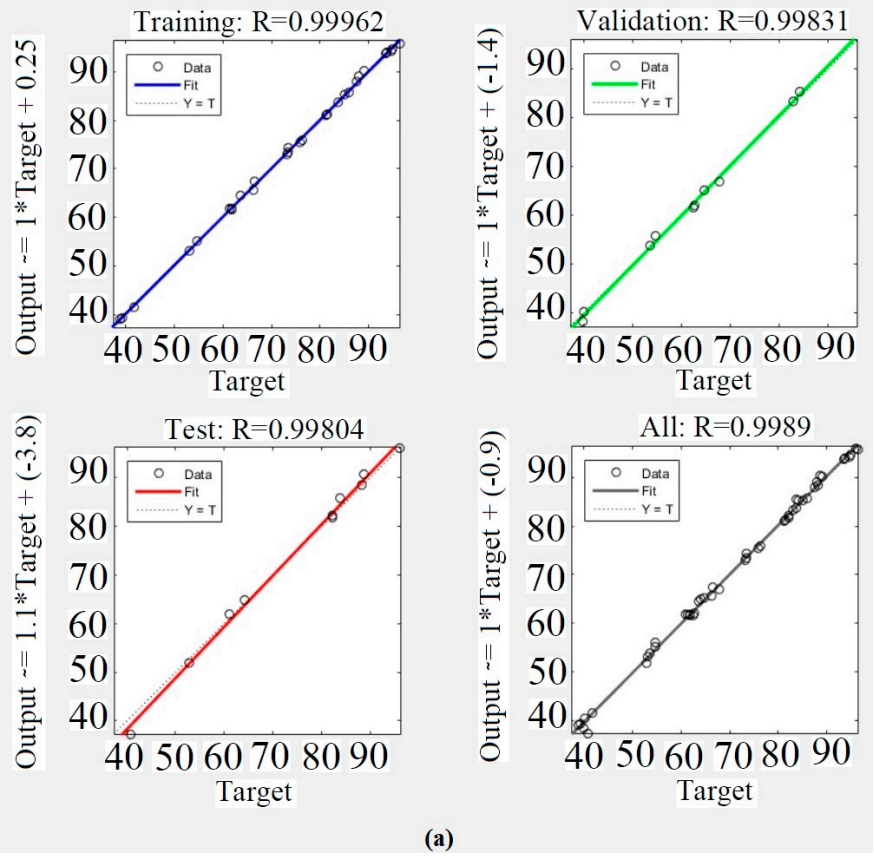

Figure 9. *Cont*.

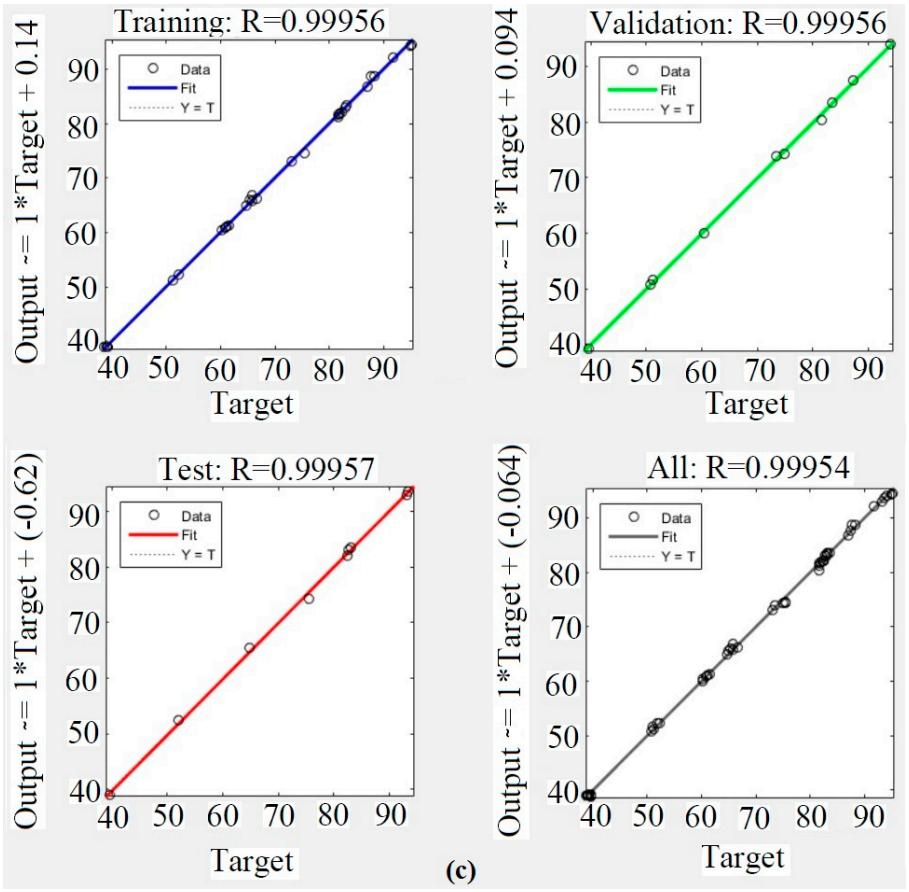

Figure 9. Model prediction versus experimental values for the optimum topology for diclofenac (**a**), ibuprofen (**b**), and naproxen (**c**).

3.3. Adsorption Isotherm

3.3.1. Langmuir Isotherm

The mathematical expression of this isotherm is presented in the following Equation (5):

$$\frac{x}{m} = \frac{abC_e}{(1 + bC_e)}, \quad (5)$$

where $\frac{x}{m}$ corresponds the mass of adsorbate adsorbed/unit mass of adsorbent (mg adsorbate per g adsorbent), a and b denote empirical constants, and C_e denotes the equilibrium concentration of the adsorbate in the solution following adsorption (mg/L) [27].

Table 4 and Figure 10 display the details of the Langmuir isotherm studies. The R^2 values were 0.932, 0.962, and 0.893 for DCF, IBP, and NPX removal, respectively. Based on Figure 10, with the decrease in values of $(1/C_e)$, the values of $(1/(x/m))$ were increased. The high R^2 values show that elimination of DCF, IBP, and NPX could be explained by the Langmuir isotherm. For the DCF elimination using the Langmuir isotherm model, the values of *b* and Q (mg/g) were 0.77 and 22.1, respectively. Jodeh et al. [45] reported Q = 22.2 during DCF removal using an adsorption method. For IBP removal using the Langmuir isotherm model, the values of *b* and Q (mg/g) were 0.64 and 21.2, respectively. For NPX elimination using the Langmuir isotherm model, the values of b and Q (mg/g) were 0.76 and 33.3, respectively. Values of Q_m = 21.7, b = 0.75, and R^2 = 0.8 were reported by Sun et al. [11] and are in line with the results of the current study. Sun et al. [11] reported Q_m = 33.6, b = 0.75 and R^2 = 0.97 during NPX removal via an adsorption method, which are also in line with the results of the current study.

Table 4. Langmuir and Freundlich isotherms study for DCF, IBP, and NPX removal by CMCAB.

Parameters	Langmuir Isotherm			Freundlich Isotherm		
	Q_m (mg/g)	b (L/mg)	R^2	K_f (mg/g(L/mg)$^{1/n}$)	1/n	R^2
DCF	22.1	0.772	0.932	30.27	−4.26	0.943
IBP	21.2	0.643	0.962	54.57	−3.75	0.934
NPX	33.3	0.765	0.893	16.94	−3.03	0.988

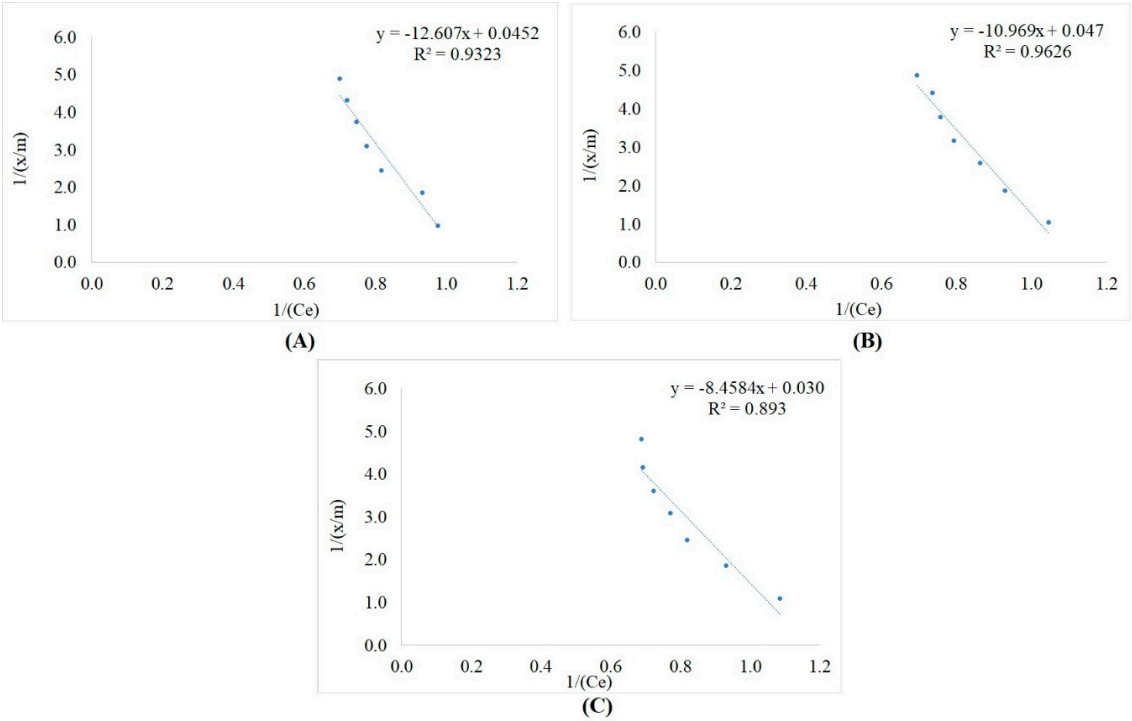

Figure 10. Langmuir isotherm regressions for diclofenac (**A**), ibuprofen (**B**), and naproxen (**C**).

3.3.2. Freundlich Isotherm

The Freundlich isotherm defines the adsorption equilibrium as follows (Equation (6)):

$$q_m = K_f C_e^{1/n} \quad (6)$$

where K_f is a fixed variable representing the relative adsorption capability of the adsorbent ($mg^{1-(1/n)}/L^{1/n}/g^{-1}$), and n is a fixed variable signifying adsorption intensity [27].

Table 4 and Figure 11 display the details of the Freundlich isotherm studies. The R^2 values were 0.943, 0.934, and 0.988 for DCF, IBP, and NPX removal, respectively. The high R^2 values show that removal of DCF, IBP, and NPX could fit the Freundlich isotherm. Based on Figure 11, with the increase in values of Log(C_e), the values of Log(x/m) were decreased.

The Freundlich capacity factor (K) and 1/n were 30.27 and −17.27, respectively, for DCF removal. Values of K_f in the range 7.6–63.6 and R^2 in the range 0.92–0.96 were reported by Sathishkumar et al. [46] for DCF removal via an adsorption method. The Freundlich capacity factor (K) and 1/n were 54.57 and −19.41, respectively, for IBP removal. Coimbra et al. [47] reported a K_f value of 55.30 and R^2 of 0.98 for IBP removal by an adsorption method. The Freundlich capacity factor (K) and 1/n were 16.94 and −12.26, respectively, for NPX removal. Mojiri et al. [48] stated that higher 1/n values indicate that the adsorption bond is weak. Increasing the log (C_e) caused decreasing the $\log\left(\frac{x}{m}\right)$. Thus, $1/n$ (the slope of the line) is negative [48].

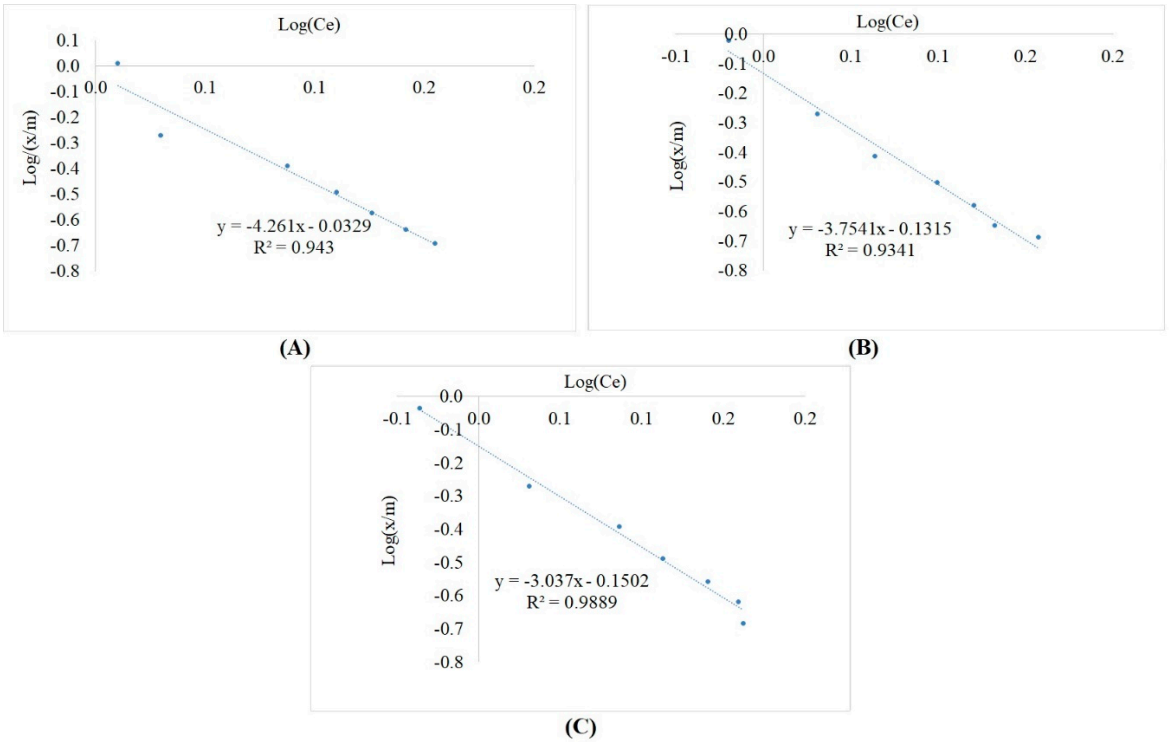

Figure 11. Freundlich isotherm regressions for diclofenac (**A**), ibuprofen (**B**), and naproxen (**C**).

3.4. Regeneration and Desorption Study

Regeneration of adsorbents is a vital procedure in wastewater treatment to decrease the processing cost. Various regeneration methods have been applied for desorption studies, including thermal regeneration and chemical regeneration. Nevertheless, it is vital to select the appropriate pH and desorbents (such as inorganic desorbents NaOH, H_2SO_4, and HCl or organic desorbents ethanol, methanol, and acetic acid) for the chemical desorption procedure [49]. Emerging micropollutants are highly soluble in alcohols due to the presence of hydroxyl groups. Moreover, the low molecular weight alcohols may enrich the effectiveness of emerging micropollutants desorption. Alizadeh Fard and Barkdoll [50] stated that NaOH and HCl could not efficiently desorb micropollutants. In addition, they also stated that methanol's restoration capacity is higher than ethanol's. In this study, after eight (Figure 12) cycles with an initial concentration of 2.5 mg/L, the removal effectiveness of the cross-linked magnetic chitosan/activated biochar remained almost unaffected.

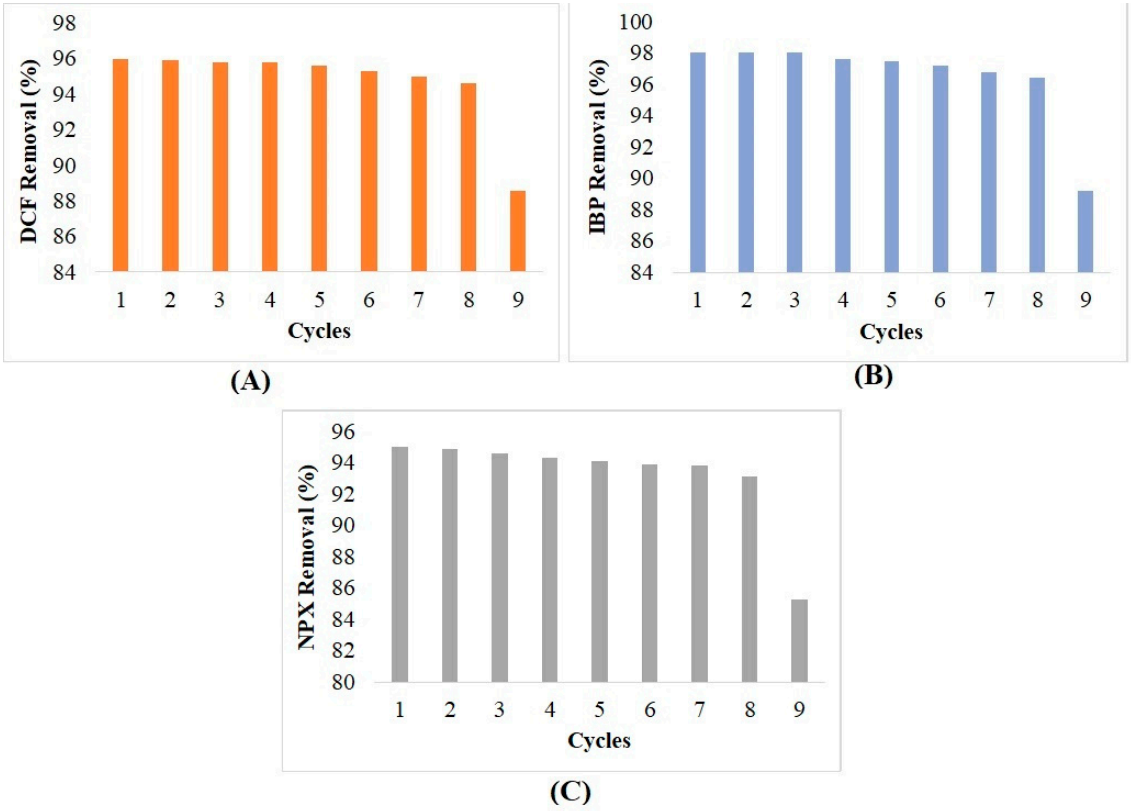

Figure 12. Regeneration results of CMCAB during removal of DCF (**A**), IBP (**B**) and NPX (**C**).

4. Conclusions

Diclofenac (DCF), ibuprofen (IBP), and naproxen (NPX) are anti-inflammatory drugs, which are a frequently consumed class of pharmaceuticals. As these are emerging micropollutants, we evaluated their removal using cross-linked magnetic chitosan/activated biochar (CMCAB). An artificial neural network (ANN) with two independent factors—pH (4–8) and micropollutant concentration (0.5–3 mg/L)—was applied to optimize the elimination efficiency. The main conclusions of this new research are listed below:

1. The optimum elimination values of DCF, IBP, and NPX were 96.4% (2.41 mg/L), 98.8% (2.47 mg/L), and 95.2% (2.38 mg/L) at pH 6.0 and an initial micropollutant concentration of 2.5 mg/L.
2. Based on the ANN, the R^2 values were 0.998, 0.998, and 0.999 for DCF, IBP, and NPX removal, indicating that optimization could be done well by an ANN.
3. Freundlich isotherm could explain the DCF and NPX removal via the CMCAB better than the Langmuir isotherm as indicated by the high R^2 values attained. But IBP removal was better fitted by Langmuir isotherm.
4. Regeneration and desorption studies indicated that CMCAB could be applied for at least eight cycles without changing the performance.

Author Contributions: A.M. was responsible for setting up the experiments, completing most of the experiments, and writing the initial draft of the manuscript; R.A.K. and A.G. modified the manuscript and contributed to the literature search.

Funding: This research received no external funding.

Acknowledgments: The author would like to express their gratitude to the Institute for Infrastructure Engineering and Sustainable Management (IIESM), University Technology Mara (UiTM), Malaysia.

Conflicts of Interest: The authors declare no conflict of interest.

References

1. Grandclement, C.; Seyssiecq, I.; Piram, A.; Wong-Wah-Chung, P.; Vanot, C.; Tiliacos, N.; Roche, N. From the conventional biological wastewater treatment to hybrid processes, the evaluation of organic micropollutant removal: A review. *Water Res.* **2017**, *111*, 297–317. [CrossRef] [PubMed]
2. Mahmoud, W.M.M.; Rastogi, T.; Kummerer, K. Application of titanium dioxide nanoparticles as a photocatalyst for the removal of micropollutants such as pharmaceuticals from water. *Curr. Opin. Green Sustain. Chem.* **2017**, *6*, 1–10. [CrossRef]
3. Landry, K.A.; Boyer, T.H. Diclofenac removal in urine using strong-base anion exchange polymer resins. *Water Res.* **2013**, *47*, 6432–6444. [CrossRef] [PubMed]
4. Wieszczycka, K.; Zembrzuska, J.; Bornikowska, J.; Wojciechowska, A.; Wojciechowska, I. Removal of naproxen from water by ionic liquid-modified polymer sorbents. *Chem. Eng. Res. Des.* **2017**, *117*, 698–705. [CrossRef]
5. Hiew, B.Y.Z.; Lee, L.Y.; Lee, X.J.; Gan, S.; Thangalazhy-Gopakumar, S.; Lim, S.S.; Pan, G.T.; Yang, T.C.K. Adsorptive removal of diclofenac by graphene oxide: Optimization, equilibrium, kinetic and thermodynamic studies. *J. Taiwan Inst. Chem. Eng.* **2018**. [CrossRef]
6. Zhang, L.; Lv, T.; Zhang, Y.; Stein, O.R.; Arias, C.A.; Brix, H.; Carvalho, P.N. Effects of constructed wetland design on ibuprofen removal—A mesocosm scale study. *Sci. Total Environ.* **2017**, 38–45. [CrossRef] [PubMed]
7. Górny, D.; Guzik, U.; Hupert-Kocurek, K.; Wojcieszyńska, D. Naproxen ecotoxicity and biodegradation by Bacillus thuringiensis B1(2015b) strain. *Ecotoxicol. Environ. Saf.* **2019**, *167*, 505–512. [CrossRef] [PubMed]
8. Amouzgar, P.; Salamatinia, B. A Short Review on Presence of Pharmaceuticals in Water Bodies and the Potential of Chitosan and Chitosan Derivatives for Elimination of Pharmaceuticals. *J. Mol. Genet. Med.* **2015**, *S4*, 001. [CrossRef]
9. Kim, E.; Jung, C.; Han, J.; Her, N.; Park, C.M.; Jang, M.; Son, A.; Yoon, Y. Sorptive removal of selected emerging contaminants using biochar in aqueous solution. *J. Ind. Eng. Chem.* **2016**, *36*, 364–371. [CrossRef]
10. Lahti, M.; Oikari, A. Microbial Transformation of Pharmaceuticals Naproxen, Bisoprolol, and Diclofenac in Aerobic and Anaerobic Environments. *Arch. Environ. Contam. Toxicol.* **2011**, *61*, 202–210. [CrossRef]
11. Sun, W.; Li, H.; Li, H.; Li, S.; Cao, X. Adsorption mechanisms of ibuprofen and naproxen to UiO-66 and UiO-66-NH2: Batch experiment and DFT calculation. *Chem. Eng. J.* **2019**, *360*, 645–653. [CrossRef]
12. Yang, Z.; Miao, H.; Rui, Z.; Ji, H. Enhanced Formaldehyde Removal from Air Using Fully Biodegradable Chitosan Grafted β-Cyclodextrin Adsorbent with Weak Chemical Interaction. *Polymers* **2019**, *11*, 276. [CrossRef]
13. Cha, J.S.; Park, S.H.; Jung, S.C.; Ryu, C.; Jeon, J.K.; Shin, M.C.; Park, Y.K. Production and utilization of biochar: A review. *J. Ind. Eng. Chem.* **2016**, *40*, 1–15. [CrossRef]
14. Quesada, H.B.; Alves Baptista, A.T.; Cusioli, L.F.; Seibert, D.; de Oliveira Bezerra, C.; Bergamasco, R. Surface water pollution by pharmaceuticals and an alternative of removal by low-cost adsorbents: A review. *Chemosphere* **2019**, *222*, 766–780. [CrossRef]
15. Sizmur, T.; Fresno, T.; Akgül, G.; Frost, H.; Moreno Jiménez, E. Biochar modification to enhance sorption of inorganics from water. *Biores. Technol.* **2017**, *246*, 34–47. [CrossRef]
16. Liu, S.; Huang, B.; Chai, L.; Liu, Y.; Zeng, G.; Wang, X.; Zeng, W.; Shang, M.; Deng, J.; Zhou, Z. Enhancement of As (V) adsorption from aqueous solution by a magnetic chitosan/biochar composite. *RSC Adv.* **2017**, *7*, 10891–10900. [CrossRef]
17. Kim, S.; Park, C.M.; Jang, A.; Hernández-Maldonadoe, A.J.; Yu, M.; Heo, J.; Yoon, Y. Removal of selected pharmaceuticals in an ultrafiltration-activated biochar hybrid system. *J. Membr. Sci.* **2019**, *570*, 77–84. [CrossRef]
18. Sühnholz, S.; Kopinke, F.D.; Weiner, B. Hydrothermal treatment for regeneration of activated carbon loaded with organic micropollutants. *Sci. Total Environ.* **2018**, 854–861. [CrossRef]
19. Lonappan, L.; Rouissi, T.; Liu, Y.; Brar, S.K.; Surampalli, R.Y. Removal of diclofenac using microbiochar fixed-bed column bioreactor. *J. Environ. Chem. Eng.* **2019**, *7*, 102894. [CrossRef]
20. Zhang, D.Q.; Hua, T.; Gersberg, R.M.; Zhu, J.; Ng, W.J.; Tan, S.K. Carbamazepine and naproxen: Fate in wetland mesocosms planted with Scirpus validus. *Chemosphere* **2013**, *91*, 14–21. [CrossRef]
21. Song, S.; Su, Y.; Adeleye, A.S.; Zhang, Y.; Zhou, X. Optimal design and characterization of sulfide-modified nanoscale zerovalent iron for diclofenac removal. *Appl. Catal. B Environ.* **2017**, *201*, 211–220. [CrossRef]

22. Wu, H.; Feng, Q.; Yang, H.; Alam, E.; Gao, B.; Gu, D. Modified biochar supported Ag/Fe nanoparticles used for removal of cephalexin in solution: Characterization, kinetics and mechanisms. *Coll. Surf. Physicochem. Eng. Asp.* **2017**, *517*, 63–71. [CrossRef]
23. De Luna, M.D.G.; Murniatib-Budianta, W.; Rivera, K.K.P.; Arazo, R.O. Removal of sodium diclofenac from aqueous solution by adsorbents derived from cocoa pod husks. *J. Environ. Chem. Eng.* **2017**, *5*, 1465–1474. [CrossRef]
24. APHA. *Standard Methods for Examination of Water and Wastewater*, 22th ed.; American Public Health Association: Washington, DC, USA, 2012.
25. Madikizelaa, L.M.; Luke Chimuka, L. Synthesis, adsorption and selectivity studies of a polymer imprinted with naproxen, ibuprofen and diclofenac. *J. Environ. Chem. Eng.* **2016**, *4*, 4029–4037. [CrossRef]
26. Tanzifi, M.; Hosseini, S.H.; Kiadehi, A.D.; Olazar, M.; Karimipour, K.; Rezaiemehr, R.; Ali, I. Artificial neural network optimization for methyl orange adsorption onto polyaniline nano-adsorbent: Kinetic, isotherm and thermodynamic studies. *J. Mol. Liq.* **2017**, *244*, 189–200. [CrossRef]
27. Mojiri, A.; Ohashi, A.; Ozaki, N.; Shoiful, A.; Kindaichi, T. Pollutant Removal from Synthetic Aqueous Solutions with a Combined Electrochemical Oxidation and Adsorption Method. *Int. J. Environ. Res. Public Health* **2018**, *15*, 1443. [CrossRef]
28. He, J.; Li, Y.; Cai, X.; Chen, K.; Zheng, H.; Wang, C.; Zhang, K.; Lin, D.; Kong, L.; Liu, J. Study on the removal of organic micropollutants from aqueous and ethanol solutions by HAP membranes with tunable hydrophilicity and hydrophobicity. *Chemosphere* **2017**, *174*, 380–389. [CrossRef]
29. Yasmeen, S.; Kabiraz, M.K.; Saha, B.; Qadir, M.R.; Gafur, M.A.; Masum, S.M. Chromium (VI) Ions Removal from Tannery Effluent using Chitosan-Microcrystalline Cellulose Composite as Adsorbent. *Inter. Res. J. Pure App. Chem.* **2016**, *10*, 1–14. [CrossRef]
30. Queiroz, M.F.; Melo, K.R.T.; Sabry, D.A.; Sassaki, G.L.; Rocha, H.A.O. Does the Use of Chitosan Contribute to Oxalate Kidney Stone Formation? *Mar. Drugs* **2015**, *13*, 141–158. [CrossRef]
31. Jindo, K.; Mizumoto, H.; Sawada, Y.; Sanchez-Monedero, M.A.; Sonoki, T. Physical and chemical characterization of biochars derived from different agricultural residues. *Biogeosciences* **2014**, *11*, 6613–6621. [CrossRef]
32. Yu, Z.; Zhang, X.; Huang, Y. Magnetic Chitosan–Iron (III) Hydrogel as a Fast and Reusable Adsorbent for Chromium (VI) Removal. *Ind. Eng. Chem. Res.* **2013**, *52*, 11956–11966. [CrossRef]
33. Zhang, M.M.; Liu, Y.G.; Li, T.T.; Xu, W.H.; Zheng, B.H.; Tan, X.F.; Wang, H.; Guo, Y.M.; Guo, F.Y.; Wang, S.F. Chitosan modification of magnetic biochar produced from Eichhornia crassipes for enhanced sorption of Cr (VI) from aqueous solution. *RSC Adv.* **2015**, *5*, 46955. [CrossRef]
34. Liang, X.X.; Omer, A.M.; Hu, Z.H.; Wang, Y.G.; Yu, D.; Ouyang, X.K. Efficient adsorption of diclofenac sodium from aqueous solutions using magnetic amine-functionalized chitosan. *Chemosphere* **2019**, *217*, 270–278. [CrossRef] [PubMed]
35. Lonappan, L.; Rouissi, T.; Brar, S.K.; Verma, M.; Surampalli, R.Y. Adsorption of diclofenac onto different biochar microparticles: Dataset—Characterization and dosage of biochar. *Data Brief* **2018**, *16*, 460–465. [CrossRef] [PubMed]
36. Chakraborty, P.; Show, S.; Benerjee, S.; Halder, G. Mechanistic insight into sorptive elimination of ibuprofen employing bi-directional activated biochar from sugarcane bagasse: Performance evaluation and cost estimation. *J. Environ. Chem. Eng.* **2018**, *6*, 5287–5300. [CrossRef]
37. Paradis-Tanguay, L.; Camire, A.; Renaud, M.; Chabot, B. Sorption capacities of chitosan/polyethylene oxide (PEO) electrospun nanofibers used to remove ibuprofen in water. *J. Polym. Eng.* **2018**. [CrossRef]
38. Jung, C.; Oh, J.; Yoon, Y. Removal of acetaminophen and naproxen by combined coagulation and adsorption using biochar: Influence of combined sewer overflow components. *Environ. Sci. Poll. Res.* **2015**, *22*, 10058–10069. [CrossRef]
39. Dewage, N.B.; Fowler, R.E.; Pittman, C.U., Jr.; Mohan, D.; Mlsna, T. Lead (Pb^{2+}) sorptive removal using chitosan-modified biochar: Batch and fixed-bed studies. *RSC Adv.* **2018**, *8*, 25368–25377. [CrossRef]
40. Gu, Y.; Yperman, J.; Carleer, R.; D'Haen, J.; Maggen, J.; Vanderheyden, S.; Vanppelen, K.; Garcia, R.M. Adsorption and photocatalytic removal of Ibuprofen by activated carbon impregnated with TiO_2 by UV–Vis monitoring. *Chemosphere* **2019**, *217*, 724–731. [CrossRef]

41. Rafati, L.; Ehrampoush, M.H.; Rafati, A.A.; Mokhtari, M.; Mahvi, H. Modeling of adsorption kinetic and equilibrium isotherms of naproxen onto functionalized nano-clay composite adsorbent. *J. Mol. Liq.* **2016**, *224*, 832–841. [CrossRef]
42. Besha, A.T.; Gebreyohannes, A.Y.; Tufa, R.A.; Bekele, D.N.; Curcio, E.; Giorno, L. Removal of emerging micropollutants by activated sludge process and membrane bioreactors and the effects of micropollutants on membrane fouling: A review. *J. Environ. Chem. Eng.* **2017**, *5*, 2395–2414. [CrossRef]
43. Ghaedi, A.M.; Karamipour, S.; Vafaei, A.; Baneshi, M.M.; Kiarostami, V. Optimization and modeling of simultaneous ultrasound-assisted adsorption of ternary dyes using copper oxide nanoparticles immobilized on activated carbon using response surface methodology and artificial neural network. *Ultrason. Sonochem.* **2019**, *51*, 264–280. [CrossRef]
44. Uddin, M.K.; Khan Rao, R.A.; Chandra Mouli, K.V.V. The artificial neural network and Box-Behnken design for Cu^{2+} removal by the pottery sludge from water samples: Equilibrium, kinetic and thermodynamic studies. *J. Mol. Liq.* **2018**, *266*, 617–627. [CrossRef]
45. Jodeh, S.; Abdelwahab, F.; Jaradat, N.; Warad, I.; Jodeh, W. Adsorption of diclofenac from aqueous solution using Cyclamen persicum tubers based activated carbon (CTAC). *J. Assoc. Arab Univ. Basic Appl.* **2016**, *20*, 32–38. [CrossRef]
46. Sathishkumar, P.; Arulkumar, M.; Ashokkumar, V.; Yusoff, A.R.M.; Murugesan, K.; Palvannan, T.; Salam, Z.; Nasir Ain, F.; Hadibarata, T. Modified phyto-waste Terminalia catappa fruit shells: A reusable adsorbent for the removal of micropollutant diclofenac. *RSC Adv.* **2015**, *5*, 30950–30962. [CrossRef]
47. Coimbra, R.N.; Escapa, C.; Otero, M. Adsorption Separation of Analgesic Pharmaceuticals from Ultrapure and Waste Water: Batch Studies Using a Polymeric Resin and an Activated Carbon. *Polymers* **2018**, *10*, 958. [CrossRef]
48. Mojiri, A.; Ahmad, Z.; Tajuddin, M.R.; Arshad, M.F.; Barrera, V. Molybdenum (VI) removal from aqueous solutions using bentonite and powdered cockle shell; Optimization by response surface methodology. *Glob. NEST J.* **2017**, *19*, 232–240. [CrossRef]
49. Zhou, Y.; Zhang, L.; Cheng, Z. Removal of organic pollutants from aqueous solution using agricultural wastes: A review. *J. Mol. Liq.* **2015**, *212*, 739–762. [CrossRef]
50. Alizadeh Fard, M.; Barkdoll, B. Using recyclable magnetic carbon nanotube to remove micropollutants from aqueous solutions. *J. Mol. Liq.* **2018**, *249*, 193–202. [CrossRef]